Space Optimization for Utilization of Plasmonic Effect on a P3HT-Gold Nanoparticle Photoelectrode

Ishida, Takuya
Department of Materials Physics and Chemistry, Graduate School of Engineering, Kyushu University

Katagishi, Miho
Department of Materials Physics and Chemistry, Graduate School of Engineering, Kyushu University

Takahashi, Yukina
Department of Applied Chemistry, Faculty of Engineering, Kyushu University

Yamada, Sunao
Department of Applied Chemistry, Faculty of Engineering, Kyushu University

https://hdl.handle.net/2324/7174394

出版情報：Chemistry Letters. 46 (11), pp.1612-1615, 2017-11-05. Oxford University Press
バージョン：
権利関係：

Space Optimization for Utilization of Plasmonic Effect on a P3HT-Gold Nanoparticle Photoelectrode

Takuya Ishida,[1,†] Miho Katagishi,[1] Yukina Takahashi,*[2] and Sunao Yamada*[2,3]
[1]*Department of Materials Physics and Chemistry, Graduate School of Engineering, Kyushu University, 744 Moto-oka, Nishi-ku, Fukuoka 819-0395, Japan*
[2]*Department of Applied Chemistry, Faculty of Engineering, Kyushu University, 744 Moto-oka, Nishi-ku, Fukuoka 819-0395, Japan*
[3]*Center for Future Chemistry, Kyushu University, 744 Moto-oka, Nishi-ku, Fukuoka 819-0395, Japan*
E-mail: yukina@mail.cstm.kyushu-u.ac.jp

Non-capped gold nanoparticles (AuNPs) with the diameter of 9-13 nm were electrochemically deposited on the ITO electrode, and poly(3-hexylthiophene-2,5-diyl) (P3HT) was spin-coated on the AuNP-deposited electrode. The degree of photocurrent enhancement exceeded unity when the coverages of AuNPs were below 14%, but were lower above 14%. The plasmonic effect was verified to be the major contribution at lower coverages, while the quenching effects became predominant at higher coverages. The spatial optimization (1-2 nm) between AuNP and P3HT was crucial and has been successful at 18%.

Organic thin film solar cells[1,2] are promising for the next generation solar cells, because they have potential advantages of lightness, flexibility, processability, wide-band light collection, and so on. However, improvement of the photocurrent generation efficiency is still a challenge to realize practical applications. As to the photoactive layer of the organic solar cells, the thicker film is better for collecting light, but becomes inferior due to increasing the resistance. In order to improve the effect of photoexcitation of organic layer in the organic solar cells, the use of localized surface plasmon resonance (LSPR)[3-5] of noble metal nanostructures is one of the most promising approaches recently. In fact, the locally-enhanced electromagnetic field due to LSPR has been used to improve the efficiency of photoluminescence[6-11], photoelectric conversion,[12-26] and photocatalysis[27-29] of dye molecules, organic semiconductor polymers, and so on. However, there still remain ambiguity on the correlations among the size and the deposition density of metal nanoparticles, and distance between molecule and metal nanoparticle. Especially, the quenching effect by metal nanoparticles, owing to energy and/or electron transfer[30-33] from excited molecules to metal nanoparticles,[34-38] has a serious problem on the intensity of photocurrent based on electron-transfer from the excited molecule to an electron acceptor present in the bulk. It is well known that the efficiencies of Förster resonance energy transfer (FRET) and nanosurface energy transfer (NSET) vary inversely with the 6th (d^{-6})[31,36-38] and 4th (d^{-4})[32-35,37,38] power of spatial distance, respectively. In the case of Dexter-type energy transfer, electron transfer occurs at very close distance (~1 nm) because this energy transfer requires overlapping the wavefunctions for electron exchange.[30] Accordingly, the quenching efficiency profoundly depends on the distance between metal nanoparticle and molecule. Thus, it is quite important to precisely control the distance between metal nanoparticle and the molecule for optimizing the efficiency of photoelectric conversion.[18,19,23,24]

We previously reported the dependence of the coverage of citrate-capped gold nanoparticle (cit-AuNP) on the photocurrent enhancement from electropolymerized polythiophene films, and showed that there was a maximum region (coverage 14%) of deposited AuNPs (~19 nm diameter) on the photocurrent enhancement due to the incorporation of AuNPs[20], while 5% for non-capped (bare) AuNPs (~16 nm) that were electrochemically deposited on the ITO electrode.[21] Those results show that there is optimal coverage depending on the diameter and the distance between AuNP and polythiophene layer. However, the effects of both the coverage and the spatial distance on the photocurrent enhancement have not been verified.

In this paper, we fabricated the photoactive electrodes consisting of non-capped AuNPs by electrodeposition method[21] and poly(3-hexylthiophene-2,5-diyl) (P3HT) layer by spin-coating method, in order to verify the optimum coverage region, and to precisely adjust the interdistance of AuNP-P3HT. The use of non-capped AuNPs was indispensable to clarify the effects of spatial distance.

Non-capped AuNPs were electrodeposited on an indium tin oxide (ITO) electrode as follows.[21] At first, the ITO electrode was washed with water, ethanol, and acetone

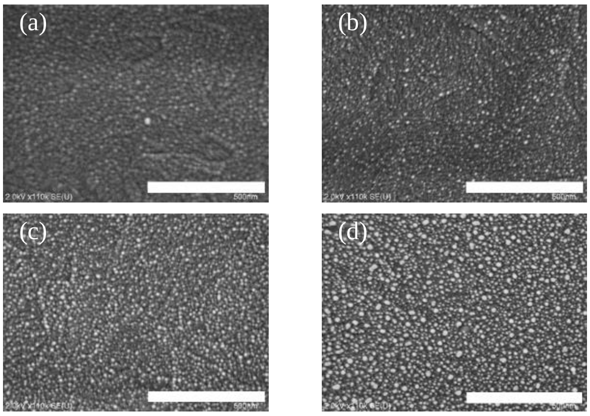

Figure 1. SEM images of the ITO/AuNP electrodes. The diameters of AuNP were 9-13 nm and the coverages of AuNP were (a) 4% (0.025 mg mL^{-1}), (b) 10% (0.050 mg mL^{-1}), (c) 18% (0.100 mg mL^{-1}), and (d) 26% (0.200 mg mL^{-1}). The scale bar is 500 nm.

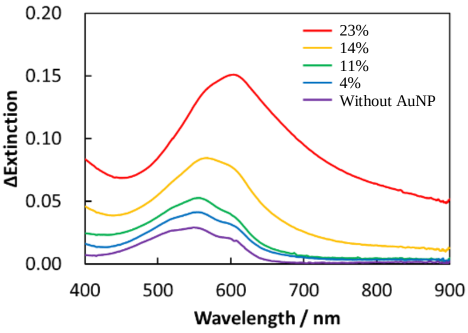

Figure 2. Differential extinction spectra of ITO/AuNP/P3HT electrodes (subtracting the absorption of ITO electrode). Blue, green, yellow, and red lines correspond to the coverage at 4, 11, 14, and 23%, respectively. Purple line is an ITO/P3HT electrode (0%).

by sonication for each 10 min, followed by ozone cleaning for 15 min. After that, the ITO electrode was immersed into an aqueous solution of HAuCl$_4$ with different concentrations (0.025, 0.050, 0.100, and 0.200 mg mL^{-1}) and the electrodeposition of AuNPs was carried out by serving an applied potential of -1.4 V vs. Ag|AgCl for 25 s, and subsequent repetition for 5 times. Reference and counter electrodes were Ag|AgCl (sat. KCl) and platinum wire, respectively. Then, the electrodeposited electrodes were annealed at 418 K for 3 h, giving the AuNP-deposited electrode denoted as ITO/AuNP. Subsequently, 50 µL of chloroform solution containing P3HT (1.0 mg mL^{-1}) was spin-coated on ITO/AuNP at 1,500 rpm and then 2,000 rpm for 10 s. Finally, the electrode was annealed at 418 K for 30 min, giving the P3HT-modified electrode, denoted as ITO/AuNP/P3HT. While, the distance between AuNP and P3HT was changed by incorporating the interlayers of polyethylenimine (PEI) alone and/or PEI and poly(styrenesulfonate) (PSS).[39] Namely, the ITO/AuNP electrode with the coverage at 18%, was immersed into an aqueous solution of PEI (45 mg mL^{-1}, 0.2 M NaCl) at 303 K for 15 min followed by rinsing with water for 15 min (ITO/AuNP/PEI), or further immersed into an aqueous solution of PSS (45 mg mL^{-1}, 0.2 M NaCl) at 303 K for 15 min, and then into the aqueous solution of PEI, with intermediate water rinsing, giving the modified electrode as: ITO/AuNP/PEI/PSS/PEI. As control samples, the P3HT layers were fabricated by spin-coating on ITO, ITO/PEI, and ITO/PEI/PSS/PEI, respectively.

Extinction and photoemission spectra of the electrodes were measured with a UV-vis-NIR spectrophotometer (UV-3150, Shimadzu) and a JASCO FP6500 spectrometer with an attachment for the measurements of solid sample (FDA-430 type; JASCO FP6000 series), respectively. Scanning electron microscopic (SEM) images were measured with Hitachi High-Tech SU8000, and the coverages of AuNP were evaluated from SEM images. Photocurrent measurements were carried out in an air-saturated aqueous solution containing Na$_2$SO$_4$ (0.10 M), methyl viologen (10 mM) using a three-electrode photoelectrochemical cell; the three electrodes were the modified one (working), Ag|AgCl (sat. KCl; reference), and platinum wire (counter). The monochromatic light from a Xe lamp irradiated to the modified electrode, and the resultant photocurrents were measured with a Huso HECS-318C potentiostat. All photocurrents were measured at 0 V (vs. Ag|AgCl).

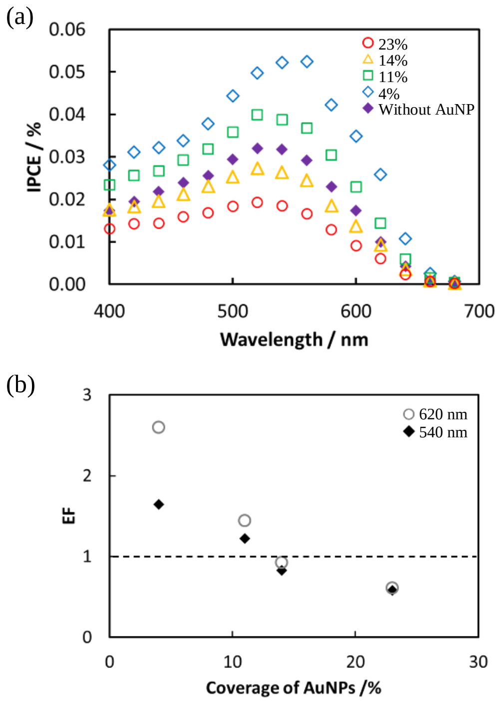

Figure 3. (a) IPCE spectra of the ITO/AuNP/P3HT electrodes in the region from 400 to 700 nm and (b) EF values at 540 and 620 nm plotted against the coverages.

It is very important to reveal detailed conditions of AuNP introduction, such as the AuNP coverage and the interdistance of AuNP-P3HT, in an organic thin film photoelectrode so as to make the most of the effects of LSPR. Thus, we have first changed the deposition density of AuNPs by changing the concentration of the aqueous solution of HAuCl$_4$. Figure 1 shows the SEM images of four kinds of ITO/AuNP electrodes with different degree of electrodeposition, where the coverages of AuNP were 4, 10, 18, and 26% with the concentrations of 0.025， 0.050， 0.100, and 0.200 mg mL^{-1}, respectively. In all cases, the diameters of AuNPs fell in 9‑13 nm. Differential extinction spectra of ITO/AuNP electrode (subtracting the extinction of ITO electrode) (Fig. S1) also showed the increase of deposition density with increasing the concentration of HAuCl$_4$ as were verified with the increase of the plasmon bands of AuNPs (550-600 nm). Similarly, differential extinction spectra of ITO/AuNP/P3HT (Fig. 2) electrodes showed the superimposition of the absorption of P3HT and

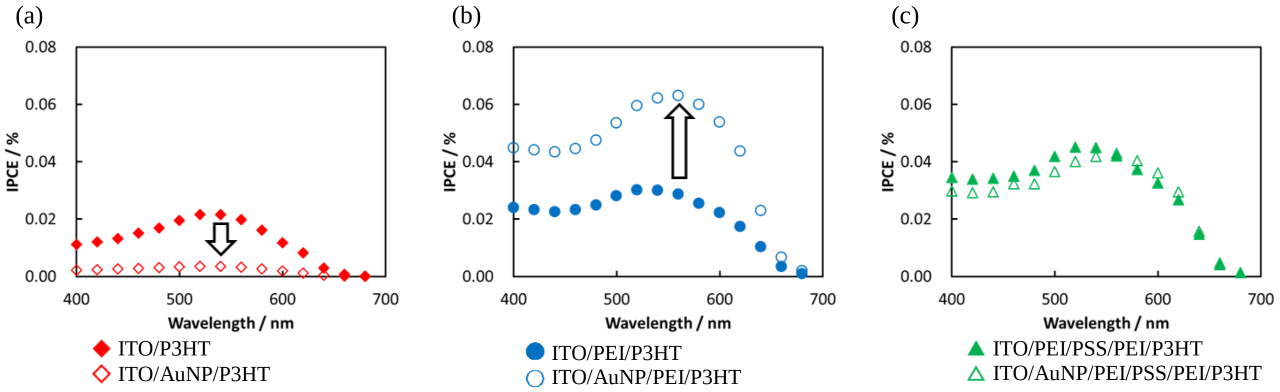

Figure 4. IPCE spectra of modified electrodes with (coverage 18%) and without AuNP.: (a) ITO/AuNP/P3HT and ITO/P3HT, (b) ITO/AuNP/PEI/P3HT and ITO/PEI/P3HT, (c) ITO/AuNP/PEI/PSS/PEI/P3HT and ITO/PEI/PSS/PEI/P3HT.

AuNPs, suggesting the almost same thicknesses of superimposed P3HT films.

IPCE spectra of the ITO/AuNP/P3HT electrodes, together with that of ITO/P3HT electrode are shown in Fig. 3a. In all cases, cathodic photocurrents were observed in the region from 400 to 700 nm based on excitation of P3HT. When the coverages of AuNP were 4% and 11%, IPCE values were larger than that of ITO/P3HT, while the values were smaller in the cases of 14 and 23%. Here, we evaluated the degree of photocurrent enhancement as an enhancement factor (EF), by dividing IPCE of the ITO/AuNP/P3HT electrode with that of the ITO/P3HT electrode, and the results are shown in Figure 3b. It was found that the EF values were larger for lower coverages of AuNP (1.7 at 540 nm (absorption of P3HT) and 2.6 at 620 nm (absorption of AuNP), at the coverage of 4%). However, the EF values were below 1.0 in the coverages 14 and 23%. In order to verify the mechanisms of enhancement and reduction of EFs, we have investigated the effects of deposition density on photoluminescence from ITO/AuNP/P3HT (Figure S2). It is clear that the order of relative intensities of photoluminescence among the five samples were roughly consistent with that in the case of IPCE values (Figure 3a). If the enhancement of photoluminescence was caused by plasmon-exciton coupling[7,11], the photocurrent, which was generated by electron-transfer from excited P3HT to viologen, must not be enhanced.[22,25] However, the photocurrents at the coverages of 4 and 11% were enhanced. The results strongly suggest that the enhancement of both photocurrent and photoluminescence at the above lower coverages was predominantly based on enhanced photoexcitation of P3HT by LSPR, and the reduction of circuit resistance due to incorporation of AuNPs was the minor contribution, if any. These enhancement effects are caused not by scattering effect but by near-field effect because, in general, small AuNPs (< 20 nm) hardly scatter the light.[40] In the case of higher coverages (14 and 23%), on the other hand, both photocurrents (Figure 3) and photoluminescence intensities (Figure S2) decreased similarly. These results can be explained by considering that the quenching effects of AuNP exceeded the enhancement effect by LSPR because of increasing the degree of close contact between AuNP and P3HT. In other words, the quenching efficiencies of FRET and NSET from excited P3HT to AuNP becomes larger with increasing the coverage of AuNPs.[11,38]

We previously reported that EF depended on the coverage of cit-AuNPs with the diameter of ~19 nm[20] and non-capped AuNPs with that of ~16 nm[21], and the maximum EF values were observed at the coverages of 14 and 5%, respectively. The existence of maximum regions in the EF values can be explained by the result of trade-off between the forward plasmonic effects and the backward quenching effects. In the present case of smaller AuNPs (9~13 nm), on the other hand, the peak of EF was not observed and EF decreased monotonically with increasing the coverage of AuNP (Figure 3b). Since the number density of AuNP is higher for smaller diameter of AuNP at the same coverage, the use of smaller AuNPs must quench the excited P3HT more effectively under the same coverage. Thus, the maximum EF value is shifted to lower coverage and the peak was not observed in this study.

Next, we investigated the effects of interdistance of AuNP-P3HT. Previous reports suggested that the efficiency of quenching effects of non-capped AuNP is higher than that of cit-capped AuNP, because P3HT can directly contact with the surface of AuNP in the former. Thus, it is fundamentally important to minimize the quenching effects, while maximizing the effects of molecular excitation by LSPR.

In order to optimize the interdistance by overcoming the above contradictory effects, we have changed the interdistance by incorporating the polymer layers between P3HT and AuNP, using alternate layer-by-layer deposition technique of polyions.[39] As a result, we have fabricated the samples of ITO/AuNP/P3HT, ITO/AuNP/PEI/P3HT and ITO/AuNP/PEI/PSS/PEI/P3HT, together with the corresponding control samples without AuNP, where the coverages of AuNPs were almost constant (~18%) in all samples. IPCE spectra of those electrode with and without polyion layers are shown in Figure. 4. The ITO/AuNP/P3HT electrode showed lower IPCE values than the ITO/P3HT one (Figure. 4a), indicating the higher quenching effects at the coverage of 18%. On the other hand, the ITO/AuNP/PEI/P3HT electrode exhibited considerably larger IPCE values as compared with the ITO/PEI/P3HT one (Fig. 4b), where the thickness of the PEI layer is estimated to be 1-2 nm (estimated from AFM: Figure S3). These results indicated that the incorporation of the PEI layer as a spacer remarkably inhibits the quenching effects of photoexcited P3HT by AuNP, while the enhancement effect based on LSPR of AuNPs can still function to the photoinduced electron-transfer leading photocurrent generation. However, the incorporation of much thicker polyion layer (PEI/PSS/PEI: 3-4 nm, See supporting information) resulted in no appreciable increase nor decrease of IPCE value as compared the electrode without AuNPs (Figure 4c). These results suggest that there is an optimum spatial distance between non-capped AuNP and P3HT for photocurrent enhancement.

In conclusion, we have carefully investigated the effects of the AuNP coverage and the distance between AuNP and P3HT on photocurrent generation. The photocurrent of the ITO/AuNP/P3HT electrode showed the EF value of 2.6 at lower coverage based on plasmonic effects, while the EF value decreased with increasing the coverage due to the increased quenching effect. In order to avoid such quenching effects, 1-2 nm) of AuNP-P3HT interdistance was quite effective even at a higher coverage (18%), by retarding the quenching effect, while utilizing the plasmonic enhancement effect. Accordingly, we have first verified the optimum adjustment of interdistane of AuNP-P3HT, in order to make the most of plasmonic effect.

This work was supported by Grants-in-Aid for Young Scientists (A) (for YT 16H06120) and Exploratory Research (for YT 16K14547) from JSPS, and the research grant of Yazaki Memorial Foundation for Science and Technology.

References and Notes

1 C. W. Tang, *Appl. Phys. Lett.* **1986**, *48*, 183.
2 M. Hiramoto, H. Fujiwara, M. Yokoyama, *Appl. Phys. Lett.* **1991**, *58*, 1062.
3 K. L. Kelly, E. Coronado, L. L. Zhao, G. C. Schatz, *J. Phys. Chem. B* **2003**, *107*, 668.
4 V. Myroshnychenko, J. R.-Fernández, I. P.-Santos, A. M. Funston, C. Novo, P. Mulvaney, L. M. L.-Marzán and F. J. García de Abajo, *Chem. Soc. Rev.* **2008**, *37*, 1792.
5 H. A. Atwater, A. Polman, *Nat. Mater.* **2010**, *9*, 205.
6 A. Wokaun, H.-P. Lutz, A. P. King, U. P. Wild, R. R. Ernst, *J. Chem. Phys.* **1983**, *79*, 509.
7 T. Okamoto, F. H'Dhili, S. Kawata, *Appl. Phys. Lett.* **2004**, *85*, 3968.
8 H. Tanaka, M. Mitsuishi, T. Miyashita, *Chem. Lett.* **2005**, *34*, 9, 1246.
9 P. Anger, P. Bharadwaj, L. Novotny, *Phys. Rev. Lett.* **2006**, *96*, 113002.
10 K. Sugawa, T. Kawahara, T. Akiyama, M. Kobayashi, A. Takahara, S. Yamada, *Chem. Lett.* **2009**, *38*, 326.
11 D. Kim, H. Yokota, T. Taniguchi, M. Nakayama, *J. Appl. Phys.* **2013**, *114*, 154307.
12 Y. Kuwahara, T. Akiyama, S. Yamada, *Langmuir* **2001**, *17*, 5714.
13 P. Peumans, A. Yakimov, S. R. Forrest, *J. Appl. Phys.* **2003**, *93*, 3693.
14 B. P. Rand, P. Peumans, S. R. Forrest, *J. Appl. Phys.* **2004**, *96*, 7519.
15 T. Akiyama, K. Inoue, Y. Kuwahara, Y. Niidome, N. Terasaki, S. Nitahara, S. Yamada, *Langmuir* **2005**, *21*, 793.
16 T. Akiyama, M. Nakada, N. Terasaki, S. Yamada, *Chem. Commun.* **2006**, 395.
17 T. Arakawa, T. Munaoka, T. Akiyama, S. Yamada, *J. Phys. Chem. C* **2009**, *113*, 11830.
18 S. D. Standridge, G. C. Schatz, J. T. Hupp, *J. Am. Chem. Soc.* **2009**, *131*, 8407.
19 T. Kawawaki, Y. Takahashi, T. Tatsuma, *Nanoscale* **2011**, *3*, 2865.
20 Y. Takahashi, S. Taura, T. Akiyama, S. Yamada, *Langmuir* **2012**, *28*, 9155.
21 Y. Takahashi, H. Umino, S. Taura, S. Yamada, *RCP* **2013**, *2*, 79.
22 R. Matsumoto, H. Yonemura, S. Yamada, *J. Phys. Chem. C* **2013**, *117*, 2486.
23 T. Kawawaki, T. Tatsuma, *Phys. Chem. Chem. Phys.* **2013**,*15*, 20247.
24 A. Kogo, Y. Takahashi, N. Sakai, T. Tatsuma, *Nanoscale* **2013**, *5*, 7855.
25 J. You, K. Leonard, Y. Takahashi, H. Yonemura, S. Yamada, *Phys. Chem. Chem. Phys.* **2014**, *16*, 1166.
26 K. Sugawa, K. Uchida, N. Takeshima, S. Jin, N. Tsunenari, H. Takeda, Y. Kida, T. Akiyama, J. Otsuki, K. Takase, S. Yamada, *Nanoscale* **2016**, *8*, 15467.
27 K. Awazu, M. Fujimaki, C. Rockstuhl, J. Tominaga, H. Murakami, Y. Ohki, N. Yoshida, T. Watanabe, *J. Am. Chem. Soc.* **2008**, *130*, 1676.
28 T. Torimoto, H. Horibe, T. Kameyama, K. Okazaki, S. Ikeda, M. Matsumura, A. Ishikawa, and H. Ishihara, *J. Phys. Chem. Lett.* **2011**, *2*, 2057.
29 T. Takahashi, A. Kudo, S. Kuwabata, A. Ishikawa, H. Ishihara, Y. Tsuboi, T. Torimoto, *J. Phys. Chem. C* **2013**, 117, 2511.
30 D. L. Dexter, *J. Chem. Phys.* **1953**, *21*, 836.
31 T. Főrster, *Discuss. Faraday Soc.* **1959**, *27*, 7.
32 R. R. Chance, A. Prock and R. Silbey, *Adv. Chem. Phys.* **1978**, *37*, 1.
33 B. N. J. Persson, N. D. Lang, *Phys. Rev. B* **1982**, *26*, 5409.
34 C. S. Yun, A. Javier, T. Jennings, M. Fisher, S. Hira, S. Peterson, B. Hopkins, N. O. Reich, G. F. Strouse, *J. Am. Chem. Soc.* **2005**, *127*, 3115.
35 T. L. Jennings, M. P. Singh, G. F. Strouse, *J. Am. Chem. Soc.* **2006**, *128*, 5462.
36 K. K. Haldar, T. Sen, A. Patra, *J. Phys. Chem. C* **2010**, *114*, 4869.
37 M. Li, S. K. Cushing, Q. Wang, X. Shi, L. A. Hornak, Z. Hong, N. Wu, *J. Phys. Chem. Lett.* **2011**, *2*, 2125.
38 X. Zhang, C. A. Marocico, M. Lunz, V. A. Gerard, Y. K. Gun'ko, V. Lesnyak, N. Gaponik, A. S. Susha, A. L. Rogach, A. L. Bradley, *ACS Nano* **2012**, *6*, 9283.
39 G. Decher, *Science* **1997**, *277*, 1232.
40 C. Deeb, X. Zhou, J. Plain, G. P. Wiederrecht, R. Bachelot, *J. Phys. Chem. C* **2013**, *117*,10669.

† Present affiliation: Institute of Industrial Science, the University of Tokyo, 4-6-1 Komaba, Meguro-ku, Tokyo 153-8505, Japan

NOTE *The diagram is acceptable in a colored form. Publication of the colored G.A. is free of charge.*
For publication, electronic data of the colored G.A. should be submitted. Preferred data format is EPS, PS, CDX, PPT, and TIFF.
If the data of your G.A. is "bit-mapped image" data (not "vector data"), note that its print-resolution should be 300 dpi.

You are requested to put a brief abstract (50-60words, one paragraph style) with the graphical abstract you provided, so that readers can easily understand what the graphic shows.

Graphical Abstract

Textual Information

A brief abstract (required)	Gold nanoparticles (AuNPs) were electrochemically deposited on the ITO electrode, and then poly(3-hexylthiophene-2,5-diyl) was coated. The degree of photocurrent enhancement exceeded unity when the coverages of AuNPs were below 14%, but was below unity above 14%. The quenching effects became predominant at higher coverages. The spatial optimization (1-2 nm) between AuNP and P3HT was crucial and has been successful at 18%.
Title(required)	Space Optimization for Utilization of Plasmonic Effect on a P3HT-Gold Nanoparticle Photoelectrode
Authors' Names(required)	Takuya Ishida, Miho Katagishi, Yukina Takahashi, and Sunao Yamada

Graphical Information